Associations between Huwe1 and autophagy in rat cerebral neuron oxygen-glucose deprivation and reperfusion injury

GUO-QIAN HE[1,2], YAN CHEN[1,3], HUI-JUAN LIAO[1,3], WEN-MING XU[1,3], WEI ZHANG[4] and GUO-LIN HE[1,5]

[1]Key Laboratory of Birth Defects and Related Diseases of Women and Children, Ministry of Education; [2]Department of Pediatrics, [3]Joint Laboratory of Reproductive Medicine, West China Second University Hospital, Sichuan University; [4]Department of Medical Oncology, Sichuan Cancer Hospital and Institute, Sichuan Cancer Center, Cancer Hospital Affiliated to School of Medicine; [5]Department of Obstetrics and Gynecology, West China Second University Hospital, Sichuan University, Chengdu, Sichuan 610041, P.R. China

Received February 11, 2019; Accepted July 15, 2020

DOI: 10.3892/mmr.2020.11611

Abstract. Autophagy and the ubiquitin proteasome system (UPS) are two major protein degradation pathways involved in brain ischemia. Autophagy can compensate for UPS impairment-induced cellular dysfunction. HECT, UBA and WWE domain containing E3 ubiquitin protein ligase 1 (Huwe1), an E3 ubiquitin ligase, serves critical roles in nervous system plasticity, regeneration and disease. However, the role of Huwe1 in autophagy in brain ischemia/reperfusion (I/R) injury remains unknown. The aim of the present study was to investigate the crosstalk between autophagy and the UPS in brain ischemia. The present study established an oxygen-glucose deprivation and reperfusion (OGD/R) model in rat primary cortex neurons *in vitro*. Lentiviral interference was used to silence the expression of Huwe1. An autophagy promoter (rapamycin), an autophagy inhibitor (wortmannin) and a JNK pathway inhibitor (SP600125) were also used in the current study. Cellular autophagy-related proteins, including Beclin-1, autophagy related (ATG) 7, ATG5, ATG3 and microtubule associated protein 1 light chain 3 α, and apoptosis-related proteins, such as P53, cleaved caspase 3, Bax and Bcl2, were detected via western blotting and immunocytochemistry. Neuronal apoptosis was evaluated using a TUNEL assay. The results demonstrated that silencing Huwe1 increased the expression levels of autophagy-related proteins at 24 h after OGD/R. Treatment with a JNK inhibitor or cotreatment with Huwe1 shRNA significantly increased autophagy. Rapamycin increased apoptosis under OGD/R conditions. However, treatment with Huwe1 shRNA decreased the number of TUNEL-positive cells at 24 h after OGD/R. Cotreatment with Huwe1 shRNA and wortmannin alleviated neuronal apoptosis under OGD/R conditions compared with cotreatment with DMSO. Collectively, the present results suggested that silencing Huwe1 was accompanied by a compensatory induction of autophagy under OGD/R conditions. Furthermore, the JNK pathway may be a key mediator of the interaction between Huwe1 and autophagy in response to UPS impairment.

Correspondence to: Dr Wei Zhang, Department of Medical Oncology, Sichuan Cancer Hospital and Institute, Sichuan Cancer Center, Cancer Hospital Affiliated to School of Medicine, 55 South Renmin Road, Chengdu, Sichuan 610041, P.R. China
E-mail: zw493493@163.com

Dr Guo-Lin He, Department of Obstetrics and Gynecology, West China Second University Hospital, Sichuan University, 20 South Renmin Road, Chengdu, Sichuan 610041, P.R. China
E-mail: heguolin19@163.com

Abbreviations: UPS, ubiquitin proteasome system; I/R, ischemia/reperfusion injury; OGD/R, Oxygen-glucose deprivation and reperfusion

Key words: UPS, HECT, UBA and WWE domain containing E3 ubiquitin protein ligase 1, autophagy, OGD/R

Introduction

Eukaryotic cells have two major intracellular degradation pathways to maintain cellular homeostasis: The ubiquitin proteasome system (UPS) and autophagy (1). The UPS is a highly selective pathway for the degradation of misfolded, short-lived and damaged proteins. Moreover, the UPS pathway recruits the proteasome to selectively recognize and degrade ubiquitinated proteins involved in a variety of cellular functions, including cell survival and death (2,3). In contrast to the UPS, autophagy is the preferred process via which long-lived proteins and damaged cytoplasmic constituents are degraded via the autophagosome-lysosome pathway, and it is involved in cellular homeostasis and stress responses (4,5). The UPS and autophagy were initially considered to function independently of one another. However, accumulating evidence has revealed crosstalk between the two degradation pathways (6,7). Previous studies investigating this crosstalk have focused on the compensatory and complementary relationship between autophagy and the UPS (7-9). It has been shown that UPS dysfunction can activate autophagy *in vitro* in cell culture and *in vivo* in animal models via the direct or indirect modulation of proteins associated with cell survival and death (10-12). The

activation of the proteasomal degradation pathway is usually inversely correlated with autophagic degradation (7,13). Several mediators, such as P53, p62 and ubiquitin, have been predicted to link the UPS and autophagy (7,14). However, the key mediators that induce disease mechanisms remain largely unknown.

The UPS involves the cooperative action of three enzymes: Ubiquitin-activating enzyme (E1), ubiquitin-transferring enzyme (E2) and ubiquitin ligase (E3) (15). E3 ligases are major participants in the UPS system, as they are the final executioners of ubiquitin tagging (13). However, little is known regarding the E3 ligases responsible for the ubiquitination of substrates degraded by selective autophagy. Among the various E3 proteins, a major ~500 kDa protein known as HECT, UBA and WWE domain containing E3 ubiquitin protein ligase 1 (Huwe1), encodes a E5-APC terminus (HECT) domain ubiquitin ligase and has several disparate substrates, such as P53, MCL1 apoptosis regulator Bcl2 family member, cell division cycle 6, histone deacetylase 2 and N-myc (11,12). Paradoxically, two seemingly divergent effects of Huwe1, involving the increased survival and increased apoptosis, have been observed in different models, such as neurogenesis and brain cancer, depending on the cell type and context (16-18). Furthermore, Huwe1 may serve critical roles in nervous system plasticity, regeneration and disease (19). UPS dysfunction is involved in brain ischemia/reperfusion (I/R), but exerts complex and unambiguous direct and indirect effects in the context of cerebral I/R due to of its pivotal role in several intracellular pathways , such as the NF-κB, reactive oxygen species and JNK signaling pathway (20-23).

Autophagy is vital to cellular homeostasis in the brain and is increased after cerebral ischemia (24). The role of heightened autophagy in ischemic neurons is a double-edged sword (25-27). Previous reports in experimental models have revealed the beneficial effects of promoting autophagy during ischemia (24,27,28) Inversely, other studies have shown that autophagy has a detrimental role in brain ischemia, and that autophagy inhibitors can attenuate neuronal damage under cerebral ischemic conditions (29-31). Moreover, previous studies have suggested that autophagy is beneficial during ischemia, but harmful during reperfusion (26,32,33). However, the precise biological function and underlying mechanism of Huwe1 in autophagy in the context of brain ischemia is yet to be elucidated. Thus, the present study aimed to investigate the effects and of Huwe1 on autophagy and its molecular regulatory properties during oxygen-glucose deprivation and reperfusion (OGD/R). An *in vitro* rat cortical neuron model of OGD/R was established to evaluate the effects of Huwe1 and its downstream signaling cascades on autophagy.

Materials and methods

Primary cortical neuron culture. Primary cortical neurons were obtained from 45 female Sprague-Dawley rats (weight, 180-200 g; Chengdu Dashuo Laboratory Animal Co., Ltd.) at embryonic day 17. The rats were raised in quiet animal housing for 1 week, without exposure to strong light, at a temperature of 23˚C with 55% humidity, 12-h day/night cycles and free access to food and water. Cerebral cortex neurons were separated from rat brains using a standardized protocol, as described previously (34,35). The cerebral cortex was dissected from the brain and treated with 0.125% trypsin solution (Sigma-Aldrich; Merck KGaA; cat. no. T4549) and 0.05% DNase I (Sigma-Aldrich; Merck KGaA; cat. no. DN25) at 37˚C for 20 min.

Neurons were suspended in DMEM (Gibco; Thermo Fisher Scientific, Inc.) supplemented with 10% FBS (Gibco; Thermo Fisher Scientific, Inc.; cat. no. 10099-141) and filtered through a cell strainer (70 μm; BD Falcon; BD Biosciences; cat. no. 352350). The dissociated cortical cells were then plated at a density of $1.5x10^6$ cells/well in 6-well plates precoated with 0.1 mg/ml poly-D-lysine (Sigma-Aldrich; Merck KGaA; cat. no. P0899) overnight at 37˚C. The cells were maintained in neurobasal medium (Gibco; Thermo Fisher Scientific, Inc.; cat. no. 12348-017) supplemented with 2% B27 (Gibco; Thermo Fisher Scientific, Inc.; cat. no. 17504-044), 100 U/ml penicillin/streptomycin and 25 mM GlutaMax (Gibco; Thermo Fisher Scientific, Inc.; cat. no. 35050-061). The neuronal cell cultures were maintained in an incubator (5% CO_2/95% air) at 37˚C for 7-12 days *in vitro* (DIV 7-12).

All protocols were in accordance with the Care and Use of Laboratory Animals and the China Council on Animal Care and the National Institutes of Health guide for the Care and Use of Laboratory Animals (NIH Publication No. 80-23, revised 1985) (36), and were approved by the Animal Ethics Committee of Sichuan University (approval no. 2018013).

OGD/R. OGD/R was induced in primary cortical neurons as described previously (37,38). At DIV 7, primary cortical neurons were maintained in glucose-free DMEM (Gibco; Thermo Fisher Scientific, Inc.; cat. no. 11966-025) in an atmosphere of 5% CO_2 and 0.3% O_2 at 37˚C for 3 h to mimic ischemic insult (OGD). After 3 h, OGD was terminated by replacing the glucose-free DMEM with complete neurobasal medium and incubating the cultures under normoxic conditions for 24, 48 or 72 h to mimic reperfusion. Cells in the control group were treated identically, except that these cells were not exposed to OGD/R. All experiments were repeated three times independently.

Lentiviral vector construction and lentiviral infection. A lentiviral vector for silencing Huwe1 (pGIPZ system) was purchased from Open Biosystems, Inc. A third-generation pseudotype lentivirus encoding green fluorescent protein (GFP)-expressing Huwe1 short hairpin (sh)RNA (GFP-Huwe1 lentivirus) was generated as previously described (26,27). The probe sequence of the shRNA targeting the coding sequence of Huwe1 (GenBank NC_005120.4; 5'-TCTAGTAGCCAA ATTGGAG-3') was produced with a three-plasmid system via the transient transfection of 293FT cells (Invitrogen; Thermo Fisher Scientific, Inc.). The pCMVdr-8.91 and pMD2G plasmids (Invitrogen; Thermo Fisher Scientific, Inc.) were used as package systems. For lentivirus production, 293FT cells plated at 70% confluency were cotransfected with Lipofectamine® 3,000 transfection reagent (Invitrogen; Thermo Fisher Scientific, Inc.). The medium was collected 48 and 72 h after transfection, filtered through a 0.45-μm pore size filter and concentrated using ultracentrifugation at 12,000 x g for 2.5 h at 4˚C. The resulting pellets were resuspended in 150 μl PBS (pH 7.2), pooled and stored at -80˚C. The

efficiency of infection, as measured by GFP fluorescence, was >90% for the GFP-Huwe1 lentivirus. Expression of knockdown in infected 293FT cells was measured for all lentiviruses via reverse transcription-quantitative PCR (RT-qPCR) using SYBR Green as described previously (39,40).

The knockdown efficiency of the Huwe1 shRNA lentivirus was assessed in primary cortical neurons. Primary cell cultures were infected on the indicated DIV 3 by adding concentrated lentivirus and 5 μg/ml polybrene (cat. no. AL-118; Sigma-Aldrich; Merck KGaA,) to the growth medium at a multiplicity of infection of 0.5. On DIV 3, 3/4 of the culture medium was removed from the culture wells, and 100 μl Huwe1 shRNA lentivirus, 500 μl fresh normal culture medium and 5 μg/ml polybrene were added to each well of the 6-well plates. The cells were incubated for 24 h at 37˚C, the medium was changed and then the cells were continuously incubated at 37˚C for 4 days before being subjected to OGD/R. The transduction efficiency was assessed using RT-qPCR and western blot analysis of Huwe1. The scramble-GFP lentivirus was used as a control in each experiment and compared with the GFP-Huwe1 lentivirus.

Drug treatment. The autophagy promoter rapamycin (cat. no. V900930), the autophagy inhibitor wortmannin (cat. no. W1628) and a JNK inhibitor (SP600125; cat. no. S5567) were purchased from Sigma-Aldrich (Merck KGaA) and dissolved in DMSO. Rapamycin (final concentration of 100 nmol/l) or wortmannin (final concentration of 1 μM) was added to the medium at 37˚C for 24 h at the onset of reperfusion on DIV 7. On DIV 7, SP600125 (final concentration of 10 mM) was added to the medium 30 min before and throughout OGD/R at 37˚C. The cells were harvested for subsequent experiments. All cells were compared with the control group (treated with the same amount of DMSO at 37˚C for 24 h). The cells were harvested 24 h after reperfusion.

TUNEL assay. Cell apoptosis was assessed using TUNEL staining. TUNEL staining was performed using an *in situ* cell death detection kit (Roche Diagnostics; cat. no. 11684817910) in accordance with the manufacturer's instructions. Cells fixed on coverslips with 4% paraformaldehyde for 30 min at room temperature and then were treated with 0.1% Triton X-100 for 10 min at room temperature. The cells were washed with PBS and incubated with 50 μl TUNEL reaction mixture at 37˚C for 1 h. The cells were then counterstained with DAPI (1:100) for 10 min at room temperature and were visualized using an inverted fluorescence microscope (Nikon Corporation). Cells were mounted with ProLong Gold antifade reagent (Invitrogen; Thermo Fisher Scientific, Inc.). In total, ten fields at x400 magnification were randomly selected to count apoptotic cells and total cells. The apoptotic index (AI) was calculated as follows: AI = (number of apoptotic cells/total number of cells counted) x100%.

Western blotting. Extracted total proteins were incubated with cold RIPA lysis buffer (Beyotime Institute of Biotechnology). Protein samples (20-60 μg) were separated on 10 or 15% SDS-PAGE gels and blotted onto PVDF membranes (EMD Millipore). The membranes were blocked with 5% non-fat milk at room temperature for 30 min. Subsequently, the membranes were incubated with primary antibodies at 4˚C overnight. The primary antibodies were as follows: Rabbit anti-Huwe1 (1:1,000; Lifespan Biosciences, Inc.; cat. no. LS-B1359), rabbit anti-ubiquitin (1:1,000; Cell Signaling Technology, Inc.; cat. no. 3933), rabbit anti-Beclin-1 (1:1,000; Cell Signaling Technology, Inc.; cat. no. 3495), rabbit anti-autophagy related (ATG)7 (1:10,000; Abcam; cat. no. ab133528), rabbit anti-ATG3 (1:10,000; Abcam; cat. no. ab108282), rabbit anti-ATG5 (1:1,000; Abcam; cat. no. ab109490), rabbit anti-p62 (1:1,000; Cell Signaling Technology, Inc.; cat. no. 16177), rabbit anti-microtubule associated protein 1 light chain 3 α (LC3; 1:1,000; Cell Signaling Technology, Inc.; cat. no. 4108), rabbit anti-cleaved caspase 3 (1:1,000; Cell Signaling Technology, Inc.; cat. no. 9664P), rabbit anti-Bcl2 (1:500; ProteinTech Group, Inc.; cat. no. 12789-1-AP), rabbit anti-Bax (1:500; ProteinTech Group, Inc.; cat. no. 50599-2-Ig), rabbit anti-P53 (1:1,000; Abcam; cat. no. ab183544) and mouse anti-tubulin (1:10,000; Zhengneng Biotechnology; cat. no. 700608). After washing, the membrane was incubated with horseradish peroxidase-conjugated secondary antibody (1:10,000; Invitrogen; Thermo Fisher Scientific, Inc.; cat. no. A24494) for 1 h at room temperature (RT). Immunoreactivity was detected with an enhanced chemiluminescence detection reagent (EMD Millipore) on film according to the manufacturer's instructions. The optical densities of the bands were quantitatively analyzed using ImageJ software (version 1.8.0; National Institutes of Health). The protein levels were normalized to the expression of tubulin.

Immunofluorescence. Cells were seeded ($2x10^4$) on coverslips, which were placed in 24-well plates. After OGD/R treatment, the cells were fixed in 4% paraformaldehyde for 10 min at room temperature, washed three times with PBS (5 min each), treated with 0.2% Triton X-100 for 15 min, blocked with 3% BSA (Sigma-Aldrich; Merck KGaA) at 4˚C for 30 min and then incubated with primary antibodies [rabbit anti-LC3B, 1:50, ProteinTech Group, Inc., cat. no. 18725-1-AP; rabbit anti-growth associated protein 43 (Gap-43), 1:200, Cell Signaling Technology, Inc., cat. no. 8945; rabbit anti-lysosomal associated membrane protein 2 (LAMP2), 1:50, ProteinTech Group, Inc. cat. no. 10397-1-AP; and mouse anti-neuron-specific class III β-tubulin (Tuj1), 1:1,250, Chemicon International; Thermo Fisher Scientific, Inc., cat. no. MAB1637] at 4˚C overnight. The coverslips were washed and incubated with secondary antibodies (1:500) at room temperature for 2 h. The secondary antibodies included Alexa 594-labeled goat F(ab')2 anti-(mouse IgG) and Alexa 488-labeled goat F(ab')2 anti-(rabbit IgG), purchased from Invitrogen (Thermo Fisher Scientific, Inc.; cat. nos. A-21208 and A-11016). The nuclei were stained with DAPI (1:100) at room temperature for 10 min. The fluoresce images were captured on a Nikon inverted fluorescence microscope (magnification, x40) and analyzed using Image Pro Plus software (version 6.0; Media Cybernetics, Inc.) and Adobe Photoshop software (version 16.0; Adobe Systems, Inc.).

RT-qPCR. SYBR Green-based RT-qPCR was performed to examine changes in the mRNA expression of Huwe1. RNA was prepared from primary rat cortical neurons

treated as aforementioned. Total RNA was isolated using TRIzol® reagent (Invitrogen; Thermo Fisher Scientific, Inc.). Subsequently, total RNA was reverse transcribed into cDNA using a reverse transcription kit (Takara Biotechnology Co., Ltd.). The temperature protocol used for reverse transcription was as follows: 25˚C for 10 min, 42˚C for 60 min and 95˚C for 5 min. Subsequently, qPCR was performed using the ABI Prism 7500 Sequence Detection system (Thermo Fisher Scientific, Inc.). For RT-qPCR analysis, the reaction contained cDNA template (500 ng), 1 μl forward and 1 μl reverse primers and 5 μl SYBR Green I Master mix (Invitrogen; Thermo Fisher Scientific, Inc.). The following thermocycling conditions were used for qPCR: 95˚C for 60 sec; followed by 45 cycles of 95˚C for 15 sec and 60˚C for 60 sec. GAPDH was used as an internal control. The following primers were used for PCR: Huwe1 forward, 5'-CAAGTAGCCATCAGCAAG A-3' and reverse, 5'-GTCCTCCAGTTCATTCTCAA-3'; and GAPDH forward, 5'-GCCAAAAGGGTCATCATCTC-3' and reverse, 5'-GTAGAGGCAGGGATGATGTTC-3'. The mRNA levels were quantified using the $2^{-\Delta\Delta Cq}$ method and normalized to the internal reference gene GAPDH (9).

Statistical analysis. Data are presented as the mean ± SEM. Statistical analyses were performed using SPSS software (version 17.0; SPSS, Inc.). Data from different time points were compared between groups using unpaired Student's t-test (for comparisons between two groups) or one-way ANOVA followed by the Tukey's test (for comparisons of ≥3 groups). $P<0.05$ was considered to indicate a statistically significant difference. Experiments were performed at least three times.

Results

Silencing Huwe1 increases the expression of autophagy-related proteins under OGD/R conditions. OGD/R-induced neuronal injury mimics cerebral I/R injury *in vitro* and results in neuronal insult (41). In our previous study, it was found that primary cortical neuron autophagy increased at 24 h after 3 h of OGD (42). To observe the effect of the administration of treatments to interfere with autophagy, reperfusion for 24 h was selected for further study. Cortical neurons were treated with the Huwe1 shRNA lentivirus on DIV 3 and then subjected to OGD for 3 h and reperfusion for 24 h on DIV 7.

Huwe1 is a large (482 kDa) HECT ubiquitin ligase (43). It was identified that the mRNA and protein expression of Huwe1 was significantly increased at 24 h reperfusion after OGD 3 h compared with the control group (Fig. 1A-C). Compared with infection with the GFP-scramble lentivirus, infection with the Huwe1 shRNA lentivirus significantly decreased the protein and mRNA expression levels of Huwe1 at 24 h reperfusion after 3 h of OGD (Fig. 1A-C). Moreover, we used Huwe1 shRNA-treated cortex neuronal cells, and found that shRNA-Huwe1also decreased the mRNA expression of Huwe1 24 h post-transfection (Fig. S1).

Ubiquitin, an 8.5-kDa protein, is activated by E1 and then transferred to E2 before conjugation to its substrate proteins by E3 ligase (10). The results demonstrated that the expression of ubiquitin was significantly increased at 24 h reperfusion after 3 h of OGD compared with the control group (Fig. 1B and C). Moreover, compared with treatment with the GFP-scramble lentivirus, infection with the Huwe1 shRNA lentivirus significantly decreased the protein expression of ubiquitin at 24 h reperfusion after 3 h OGD.

The influence of Huwe1 on autophagy under OGD/R conditions was investigated by measuring the expression levels of autophagy-related proteins during OGD/R. A number of autophagy-related proteins have been reported to be involved in autophagy (44), such as ATG5 and LC3, which exists in two forms, LC3 I and its proteolytic derivative LC3 II. Furthermore, the conversion of LC3 I (16 kDa) to LC3 II (14 kDa) indicates 'LC3 puncta processing', and the generation of LC3 II is used to detect autophagic activity (45). The expression of autophagy-related proteins (Beclin-1, ATG7, ATG3, ATG5 and LC3-II/LC3-I) was significantly increased at 24 h reperfusion after 3 h of OGD compared with the control group. Compared with treatment with the GFP-scramble control lentivirus, infection with Huwe1 shRNA significantly decreased the expression of p62, but significantly increased the expression of ATG5 and the rate of LC3-II/LC3-I at 24 h after reperfusion (Fig. 1B and D). In addition, other autophagy-related proteins, such as Beclin-1, ATG7 and ATG3, were examined. Significantly increased expression levels of Beclin-1, ATG7 and ATG3 were identified at 24 h after reperfusion in cortical neurons treated with Huwe1 shRNA compared with those infected with the GFP-scramble control lentivirus (Fig. 1B and D). These findings indicated an enhancement of neuronal autophagy after Huwe1 silencing under OGD/R injury.

Immunofluorescence results for LAMP2. Autophagy can be divided into three types: Chaperone-mediated autophagy (CMA), microautophagy and macroautophagy. Previous studies have focused on macroautophagy under ischemic conditions, but there is evidence for the activation of CMA after ischemia and hypoxia (46-48). LAMP2 is involved in CMA (48,49). Therefore, the present study examined the expression of LAMP2 in cortical neurons using immunofluorescence, and LAMP2 was only faintly detected in the cytosolic fraction of healthy control cortical neurons (Fig. 2A). OGD/R-treated cortical neurons exhibited a significantly increased average optical value of LAMP2 at 24 h after reperfusion (Fig. 2B and E) compared with the control cortical neurons. In addition, compared with treatment of GFP-scramble control lentivirus (Fig. 2C), infection with the Huwe1 shRNA lentivirus significantly increased the average optical value of LAMP2 at 24 h after OGD (Fig. 2D and E). These results suggested that silencing Huwe1 also increased the expression of LAMP2 under OGD/R injury, as this protein is involved in CMA.

Silencing Huwe1 and inhibiting the JNK pathway affects autophagy under OGD/R conditions. The potential mechanisms underlying the regulation of Huwe1 in autophagy under OGD/R conditions were examined.

Healthy neurons in the control group developed normal polarity, exhibiting a single axon and multiple dendrites, and LC3B was at a basal level in normal neurons (Fig. 3A). Compared with these normal cortical neurons, OGD/R-treated cortical neurons exhibited a significantly increased average optical value of LC3B at 24 h after reperfusion (Fig. 3B and M).

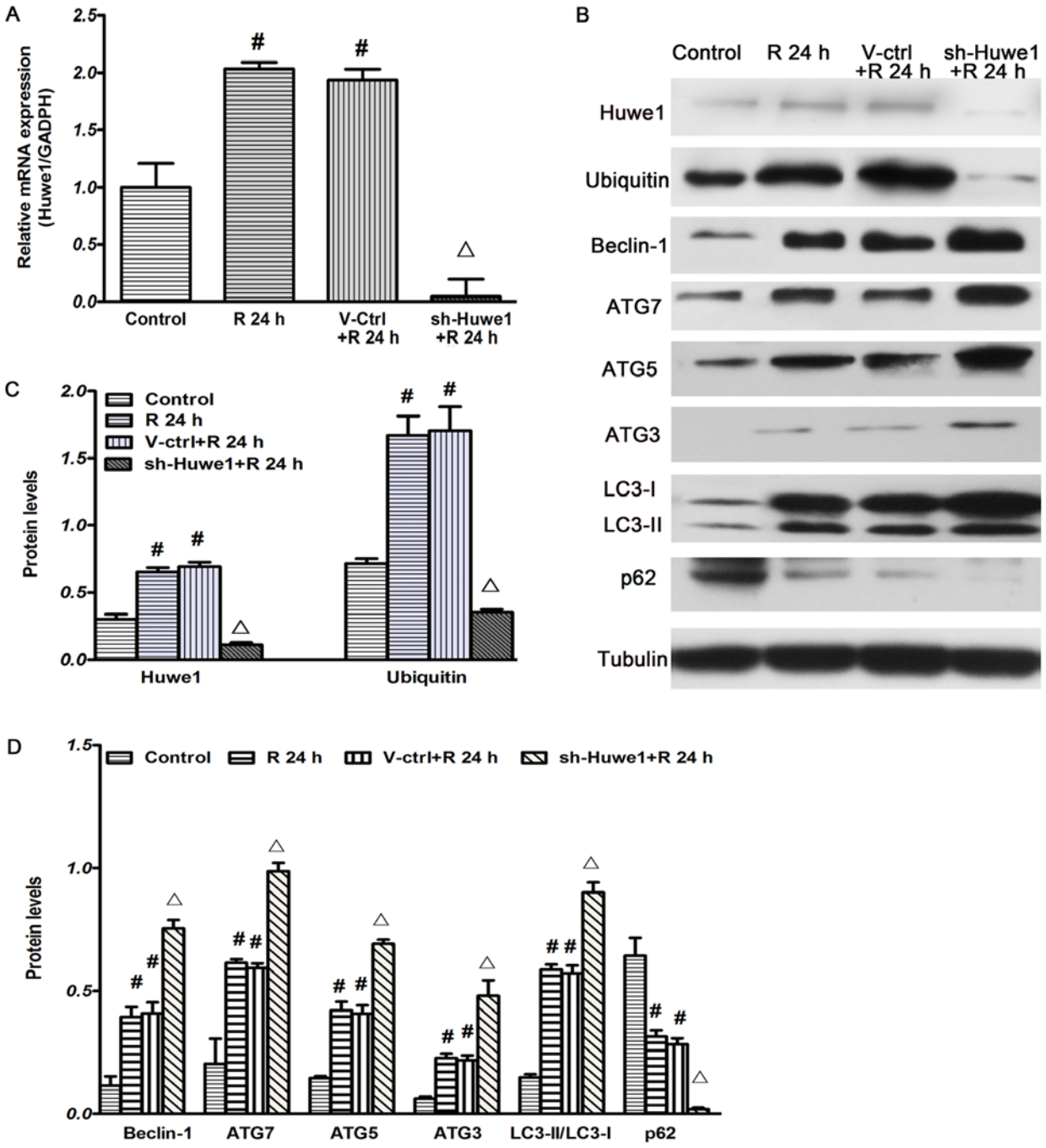

Figure 1. Silencing Huwe1 induces the expression of autophagy-related proteins under OGD/R conditions. Huwe1 shRNA lentivirus was infected into cortical neuronal cells on DIV 3, and then the cells were subjected to OGD for 3 h and reperfusion for 24 h on DIV 7. (A) Huwe1 shRNA lentivirus decreased the mRNA expression of Huwe1 at 24 h after reperfusion, as measuring via reverse transcription-quantitative PCR, with GAPDH as an internal control. (B) Huwe1 shRNA decreased the protein expression levels of (C) Huwe1 and ubiquitin at 24 h after reperfusion, but significantly increased the expression of (D) autophagy-related proteins (Beclin-1, ATG7, ATG5, ATG3 , LC3 and p62) compared with the V-ctrl group, as detected using western blotting. Tubulin was used as an internal control for western blotting. All experiments were repeated three times independently. $^{\#}$P<0.05 vs. the control group; $^{\Delta}$P<0.05 vs. the V-ctrl group. DIV, days *in vitro*; V-ctrl, green fluorescent protein-scramble control lentivirus-treated group; R, reperfusion; OGD, Oxygen-glucose deprivation; sh, short hairpin RNA; Huwe1, HECT, UBA and WWE domain containing E3 ubiquitin protein ligase 1; ATG, autophagy related; LC3, microtubule associated protein 1 light chain 3 α.

Silencing Huwe1 significantly increased the expression of LC3B at 24 h after OGD/R, compared with the scramble control (Fig. 3C, D and M). The cell body and proximal end of neurites became shortened and degraded at 24 h after OGD in the OGD/R + shRNA-Huwe1 group (Fig. 3D).

The effects of the administration of treatments to interfere with autophagy on the potential mechanisms underlying the regulation of Huwe1 in autophagy were also evaluated. Compared with DMSO (Fig. 3E), SP600125 significantly increased the expression of LC3B under OGD/R conditions at 24 h after reperfusion (Fig. 3F and M). Compared with cotreatment with DMSO and the scramble control lentivirus (Fig. 3I), cotreatment with SP600125 and Huwe1 shRNA also significantly increased the level of LC3B at 24 h and caused

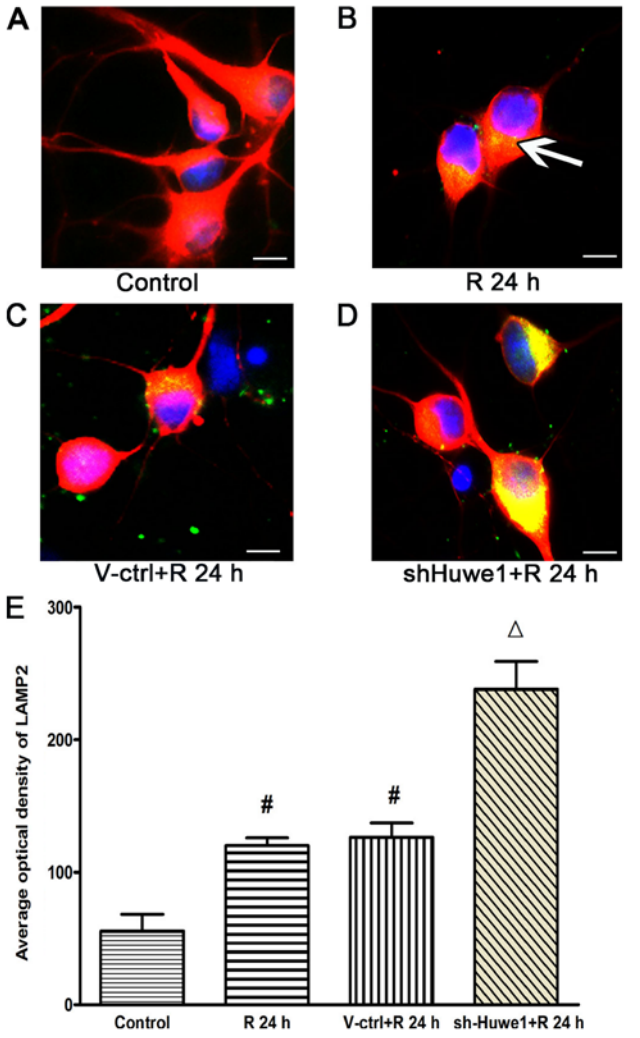

Figure 2. Silencing Huwe1 affects the expression of LAMP2, as determined via immunofluorescence. Primary cortical neurons cultured on coverslips were infected with the Huwe1 shRNA lentivirus and then exposed to OGD for 3 h and reperfusion for 24 h. Neuronal cells were stained with LAMP2 (green) and Tuj1 (red) for a double label immunofluorescence assay. DAPI (blue) was used to stain cell nuclei. LAMP2 immunofluorescence was observed mainly around the cell cytoplasm in cortical neuronal cells under (B) OGD/R conditions (indicated by white arrowheads), compared with (A) normal control cells. Compared with cells (C) treated with the GFP scramble lentivirus control, (D) infection with Huwe1 shRNA markedly increased the expression of LAMP2 at 24 h. Scale bar, 10 μm. (E) Quantification of immunofluorescence results. All experiments were repeated three times independently. $^{\#}$P<0.05 vs. control group; $^{\Delta}$P<0.05 vs. V-ctrl group. V-ctrl, green fluorescent protein-scramble control lentivirus-treated group; R, reperfusion; OGD, Oxygen-glucose deprivation; sh, short hairpin RNA; Huwe1, HECT, UBA and WWE domain containing E3 ubiquitin protein ligase 1; LAMP, lysosomal associated membrane protein 2.

neuronal cells to lose polarity (Fig. 3J and M). Rapamycin significantly enhanced the expression of LC3B at 24 h after reperfusion compared with DMSO (Fig. 3H and M). It was also found that, compared with cotreatment with DMSO and the scramble control lentivirus, cotreatment with rapamycin and Huwe1 shRNA significantly enhanced the expression of LC3B at 24 h (Fig. 3L and M), as well as caused neuronal cells to lose polarity. The autophagy inhibitor wortmannin decreased the average optical value of LC3B at 24 h after 3 h of OGD compared with DMSO treatment (Fig. 3G). Moreover, compared with cotreatment with DMSO and the scramble control lentivirus, cotreatment with wortmannin and Huwe1 shRNA inhibited the expression of LC3B at 24 h, and maintained the relatively intact structure and polarity of some neurons after OGD (Fig. 3K). Thus, a decrease in activated JNK may be involved in the effect of Huwe1 on autophagy under OGD/R injury.

Autophagy modulates hypoxia-induced apoptosis under OGD/R conditions. Autophagy triggers either apoptosis or necrotic cell death (50), and LC3, as a key molecule involved in autophagy, is required for autophagic cell death (4,24). The present study administered the autophagy promoter, rapamycin, and the autophagy inhibitor, wortmannin, under OGD/R conditions. It was demonstrated that rapamycin significantly increased the ratio of LC3-II/LC3-I at 24 h after reperfusion (Fig. 4A and C). However, wortmannin significantly decreased the ratio of LC3-II/LC3-I at 24 h after reperfusion (Fig. 4A and D).

Apoptosis is involved in DNA damage and involves various regulators of the cell cycle, including P53, Bcl2 and Bax, and the protein downstream cleaved caspase 3. Bcl2 is an anti-apoptotic protein, while Bax is a pro-apoptotic protein that belongs to the Bcl2 family of evolutionarily related proteins (51-54). The results suggested that rapamycin significantly increased the expression levels of P53, Bcl2 and cleaved caspase 3, but significantly decreased the expression of Bax at 24 h after reperfusion (Fig. 4B and E) compared with treatment with DMSO. Moreover, wortmannin significantly reduced the expression levels of P53, Bcl2 and cleaved caspase 3, but increased the expression of Bax at 24 h after reperfusion (Fig. 4B and E) compared with treatment with DMSO.

Subsequently, neurons were prepared to detect apoptosis using TUNEL staining at 24 h after OGD, and the results were quantified (Fig. 5J). An increased level of autophagy is harmful to neuronal cells in the context of OGD/R (54). OGD induced neuron cell apoptosis at 24 h compared with the control group (Fig. 5A). Compared with the scramble control lentivirus (Fig. 5B; AI, 41.29±1.82%), Huwe1 shRNA significantly decreased the number of TUNEL-positive cells (Fig. 5C; AI, 23.01±2.03%). Compared with treatment with DMSO (Fig. 5D; AI, 40.66±4.17%), treatment with wortmannin significantly decreased neuronal apoptosis at 24 h after OGD/R (Fig. 5E; AI, 21.45±8.97%). Moreover, compared with cotreatment with DMSO and the scramble control lentivirus, infection with Huwe1 shRNA and treated with wortmannin significantly decreased the number of TUNEL-positive cells (Fig. 5H; AI, 23.20±2.96%). Compared with treatment with DMSO (AI, 40.66±4.17%), treatment with SP600125 (Fig. 5F; AI, 21.34±8.05) also significantly decreased the number of TUNEL-positive cells at 24 h after OGD. The results demonstrate that, compared with cotreatment with DMSO and the scramble control lentivirus (Fig. 5G; AI, 42.05±10.07%), cotreatment with Huwe1 shRNA and SP600125 (Fig. 5I; AI, 17.15±8.25%) significantly decreased the number of TUNEL-positive cells.

Immunofluorescence results for Gap-43. Gap-43 is abundantly synthesized, especially in growth cones that are associated with axonal growth, and serves a critical role in

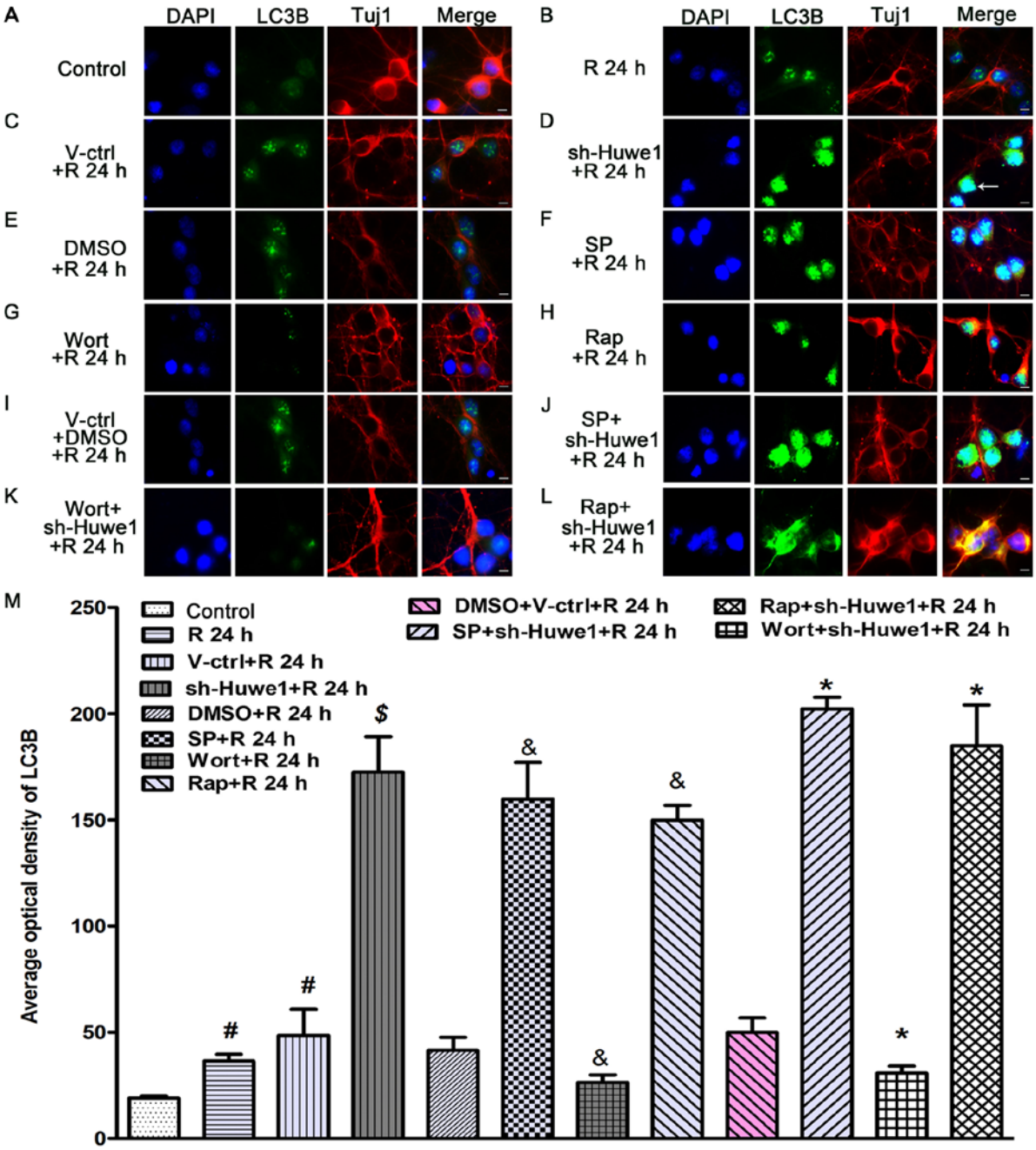

Figure 3. Immunofluorescence staining results for Tuj1 and LC3B. Cultured cortical neurons were infected with Huwe1 shRNA with or without an autophagy inhibitor, an autophagy inducer or a JNK pathway inhibitor, and then subjected to OGD/R for 24 h. Neuronal cells were stained with LC3B (green) and Tuj1 (red) for a double label immunofluorescence assay. DAPI (blue) was used to stain the cell nuclei. (A) Healthy, control neurons had normal polarity, with most of the cells having a single axon and multiple dendrites. LC3B was mainly localized to the cell nucleus in (B) cortical neuronal cells under OGD/R conditions compared with healthy control neurons. The cell bodies and proximal end of neurites became shortened and degraded at 24 h after OGD. (C) Compared with the control lentivirus, (D) treatment with Huwe1 shRNA increased the expression of LC3B. (E) Compared with DMSO, (F) the JNK inhibitor or (H) an autophagy inducer increased the expression of LC3B, as well as shortened neuronal axons at 24 h after OGD. (I) Compared with cotreatment with the control lentivirus and DMSO, (J) cotreatment with Huwe1 shRNA and a JNK inhibitor also increased the level of LC3B at 24 h. Compared with (E) DMSO, (G) Wort decreased the expression of LC3B and slightly reduced neurite degradation at 24 h after OGD. Relatively intact structure and polarity of some neurons was observed at 24 h upon (K) cotreatment with Huwe1 shRNA and Wort. (L) Cotreatment with Huwe1 shRNA and autophagy inducer also increased the level of LC3B at 24 h. Scale bar, 10 μm (magnification, x60). (M) Quantitation of the staining results. $^{\#}$P<0.05 vs. control group; $^{\$}$P<0.05 vs. V-ctrl group; $^{\&}$P<0.05 vs. DMSO group; *P<0.05 vs. the DMS + V-ctrl group. Wort, wortmannin; V-ctrl, green fluorescent protein-scramble control lentivirus-treated group; R, reperfusion; OGD, Oxygen-glucose deprivation; sh, short hairpin RNA; Huwe1, HECT, UBA and WWE domain containing E3 ubiquitin protein ligase 1; LC3, microtubule associated protein 1 light chain 3 α; Tuj1, neuron-specific class III β-tubulin; SP, SP600125; Rap, Rapamycin.

neuronal differentiation, plasticity and regeneration (55). It was identified that OGD/R increased the average optical value of Gap-43 at 24 h reperfusion after 3 h of OGD compared with normal cortical neurons (Fig. 6B). Huwe1 silencing (Fig. 6D) and the autophagy inhibitor wortmannin (Fig. 6F) also increased the average optical value of Gap-43 at 24 h reperfusion after 3 h of OGD. However, compared with cotreatment with DMSO and the scramble control lentivirus

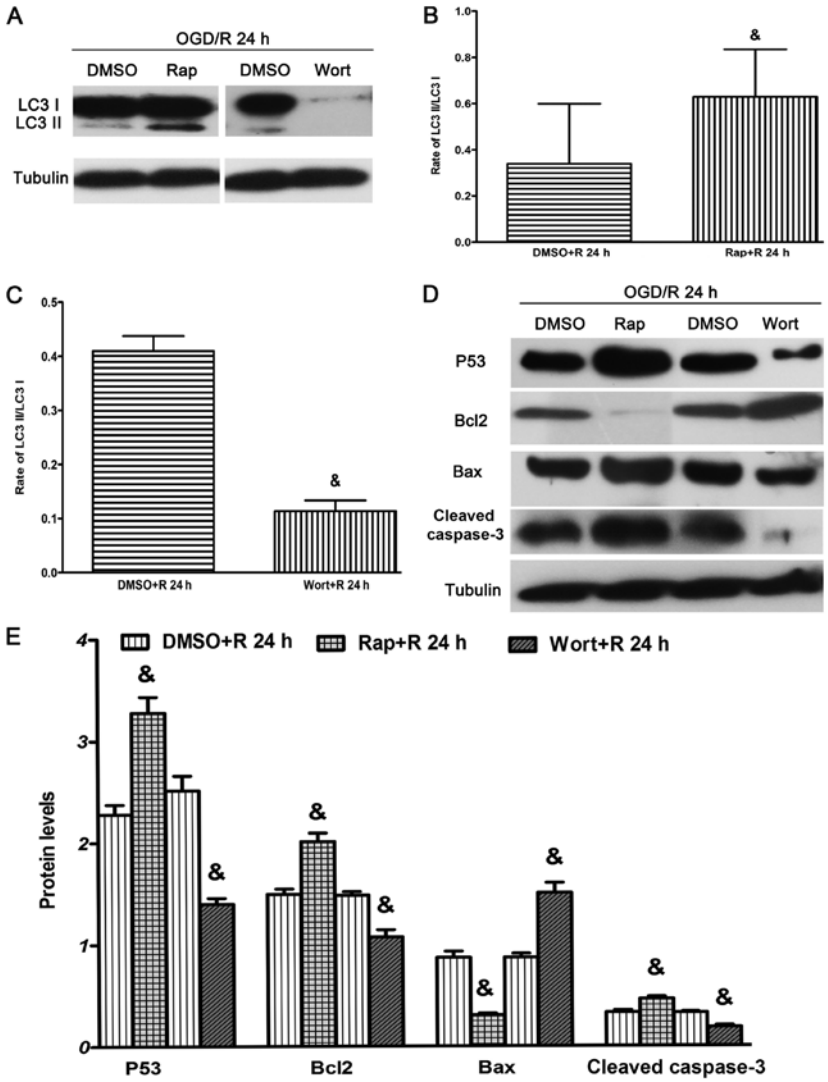

Figure 4. Treatment with an autophagy inducer or autophagy inhibitor modulates key apoptotic proteins under OGD/R conditions. Neuronal cells were treated with the autophagy inducer Rap or the autophagy inhibitor Wort at the onset of reperfusion. (A) Cells were harvested for western blot analysis of LC3 at 24 h after OGD/R. (B) Rap increased the ratio of LC3-II/LC3-I under OGD/R conditions. (C) Wort decreased the ratio of LC3-II/LC3-I. (D and E) Western blotting results of apoptosis-related proteins, P53, Bax, Bcl2 and cleaved caspase 3. Tubulin was used as an internal control. Rap increased the expression of apoptosis-related proteins. Wort decreased the protein level of apoptosis-related proteins. All experiments were repeated three times independently. $^{\&}P<0.05$ vs. DMSO group. Rap, Rapamycin; R, reperfusion; OGD, Oxygen-glucose deprivation; LC3, microtubule associated protein 1 light chain 3 α; Wort, wortmannin.

(Fig. 6G), cotreatment with wortmannin and Huwe1 shRNA did not increase the expression of Gap-43 at 24 h after OGD (Fig. 6H).

Discussion

The UPS and autophagy were previously suggested to be networks with separate components, mechanisms and substrate selectivity (13). Recently, however, studies have reported that crosstalk between autophagy and the UPS occurs at several molecular and functional sites shared between these pathway, as either regulators or substrates (7,12,56). In the present study, it was demonstrated that: i) Silencing Huwe1 induced neuronal autophagy at 24 h after OGD/R; ii) silencing Huwe1 increased neuronal autophagy via the JNK pathway under OGD/R conditions; and iii) silencing Huwe1 and inhibiting autophagy affected apoptosis at 24 h after OGD/R. Based on these findings, the present study proposed a model that involves a role for JNK in the regulation of autophagy when there is dysfunction in Huwe1 (Fig. 7).

The UPS regulates numerous cellular processes and serves a key role in various stress conditions, such as ischemia (17). Autophagy can act as a compensatory mechanism upon the impairment of proteasomal degradation (7,57,58). The UPS comprises the E1, E2 and E3 enzyme cascades. A previous study revealed that E3 ligases, including the EI24-mediated degradation of RING-domain E3 ligases, serves a critical role at the interface between the UPS and autophagy by mediating the proteasomal degradation of a subset of substrates (13). Another study observed that Huwe1 encodes a HECT domain ubiquitin ligase and is important for neurogenesis in the cerebral cortex (19). The present results suggested that silencing Huwe1 increased autophagy under OGD/R conditions.

Autophagy, closely resembling the UPS, is achieved via the combined action of several ATGs (59). Moreover,

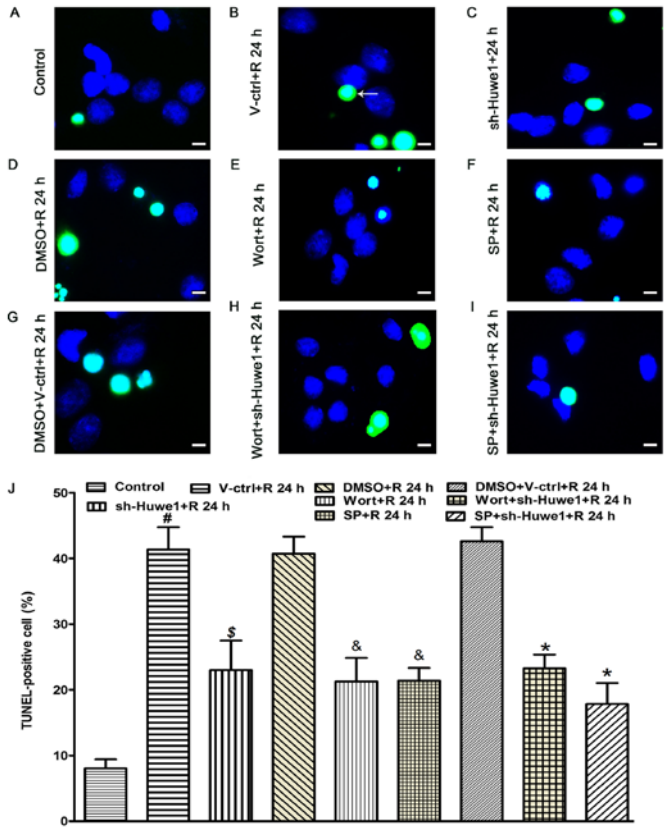

Figure 5. Apoptosis of neurons, as determined via TUNEL assay. Primary cortex neuronal cells were exposed to OGD for 3 h and reperfusion for 24 h. Neuronal cells were treated with the autophagy inhibitor Wort at the onset of reperfusion or a JNK inhibitor (SP). Apoptotic neurons were stained with TUNEL (green) for the fluorescence assay. DAPI (blue) was used to stain cell nuclei. Compared with (A) healthy control cortical neurons, TUNEL-positive cells (indicated by white arrowheads) were detected in (B) cortical neurons at 24 h after OGD. (C) Treatment with Huwe1 shRNA decreased neuronal apoptosis at 24 h after OGD. Compared with (D) DMSO treated cells, (E) Wort and a (F) JNK inhibitor reduced cellular apoptosis at 24 h after OGD. (G) Compared with the DMSO + V-ctrl group, (H) cotreatment with Huwe1 shRNA and Wortmannin also reduced cellular apoptosis at 24 h. (I) Cotreatment with Huwe1 shRNA and JNK inhibitor decreased neuronal apoptosis at 24 h. Scale bar, 10 μm. (J) Quantification of TUNEL assay results. All experiments were repeated three times independently. $^{\#}$P<0.05 vs. control group; $^{\$}$P<0.05 vs. V-ctrl group; $^{\&}$P<0.05 vs. DMSO group; *P<0.05 vs. DMSO + V-ctrl group. R, reperfusion; OGD, Oxygen-glucose deprivation; Wort, wortmannin; SP, SP600125; V-ctrl, green fluorescent protein-scramble control lentivirus-treated group; sh, short hairpin RNA; Huwe1, HECT, UBA and WWE domain containing E3 ubiquitin protein ligase 1.

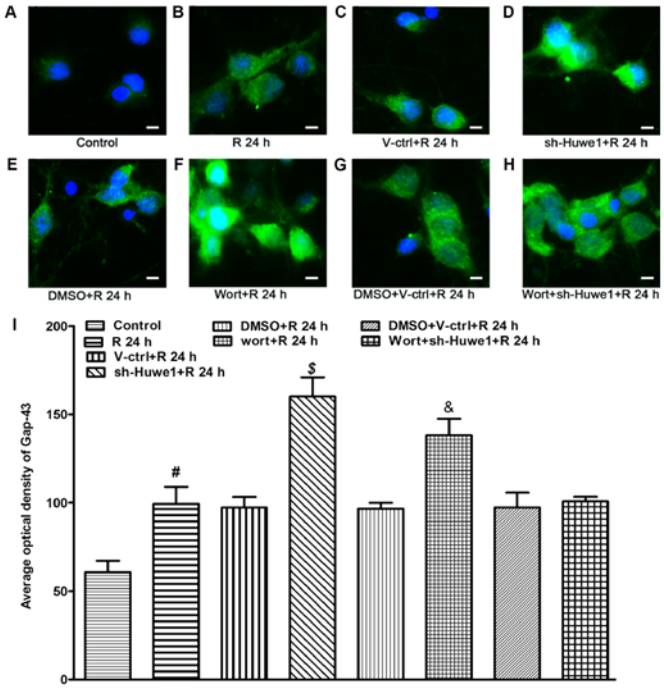

Figure 6. Immunofluorescence staining results for Gap-43. Neuronal cells were treated with Huwe1 shRNA with or without the autophagy inhibitor Wort. Neuronal cells were stained with Gap-43 (green), and DAPI (blue) was used to stain cell nuclei. (A) Compared with normal control cells, (B) the expression of Gap-43 at 24 h after OGD was increased. (C) Compared with the control lentivirus, (D) treatment with Huwe1 shRNA also increased the level of Gap-43 at 24 h. (E) Compared with DMSO, (F) an autophagy inhibitor (Wort) increased the expression of Gap-43 at 24 h. (G) Compared with cotreatment with DMSO and the green fluorescent protein scramble lentivirus, (H) cotreatment with Huwe1 shRNA and wortmannin induced the relative expression of Gap-43 at 24 h. Scale bar, 10 μm. (I) Quantitation of the staining results. All experiments were repeated three times independently. $^{\#}$P<0.05 vs. control group; $^{\$}$P<0.05 vs. V-ctrl group; $^{\&}$P<0.05 vs. DMSO group. R, reperfusion; OGD, Oxygen-glucose deprivation; Wort, wortmannin; V-ctrl, green fluorescent protein-scramble control lentivirus-treated group; sh, short hairpin RNA; Huwe1, HECT, UBA and WWE domain containing E3 ubiquitin protein ligase 1; Gap-43, growth associated protein 43.

Guo *et al* (59) demonstrated that when the UPS is impaired, autophagy is activated. In the current study, treatment with Huwe1 shRNA increased ATG7, ATG5 and ATG3 expression levels after reperfusion for 24 h. LC3-II is the cleaved form of LC3-I, and an increased LC3-II/LC3-I ratio reflects active autophagy (24,60). The ratio of LC3-II/LC3-I was also increased by treatment with shRNA-Huwe1 under OGD/R conditions in the present study, and thus the results suggested that silencing the expression of Huwe1 induced autophagy under OGD/R conditions. It was also identified that silencing Huwe1 increased the expression of LAMP2 under OGD/R conditions. Therefore, the current findings indicated that autophagy can act as a compensatory mechanism upon the impairment of the E3 ligase Huwe1. However, there is

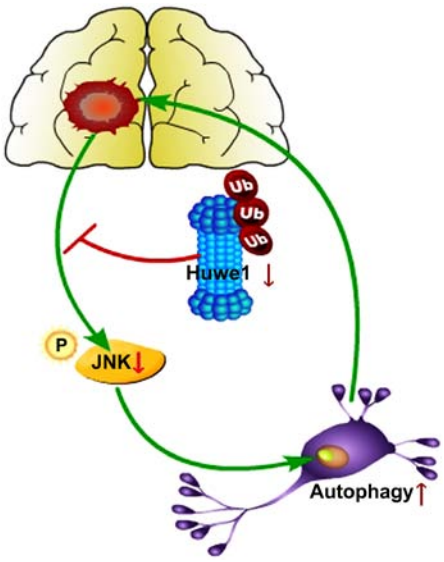

Figure 7. A compensatory mechanism of Huwe1 and autophagy exist in cortical neuron ischemia and reperfusion injury. When Huwe1 is impaired, autophagy is activated. In this process, the key modulator is p-JNK, which negatively regulates autophagy. Huwe1, HECT, UBA and WWE domain containing E3 ubiquitin protein ligase 1; p, phosphorylated.

limited evidence regarding the precise mechanism(s) of this crosstalk.

JNK is an important component of mitogen-activated protein kinase (MAPK) cascades, which serves an important role in transducing signals involved in autophagy (46,49,61-63). Our previous study also revealed that OGD/R-treated neurons exhibit decreased phosphorylation of JNK at 24 h compared with normal neuronal cells (42). Treatment with the Huwe1 shRNA lentivirus also decreases the ratio of phosphorylated-JNK/JNK upon reperfusion for 24 h after 3 h of OGD, while total JNK content is unchanged (50). Tuj1 is a somatodendritic marker of dendrites and axons, while LC3B has been used to monitor autophagy via measuring increases in punctate LC3 (61).

For example, previous studies of non-neuronal cells have implicated JNK in the induction of autophagy (64-66). In contrast to the pro-autophagic role of JNK in non-neuronal cells, neuronal JNK suppresses autophagy (67). In the current study, it was identified that the loss of neuronal JNK function caused the activation of autophagy. Moreover, the present results suggested that silencing Huwe1 decreased the phosphorylation of JNK under OGD/R conditions. It was also demonstrated that cotreatment with a JNK inhibitor and Huwe1 shRNA significantly increased the expression levels of autophagy-related proteins. Collectively, these findings indicated that increased autophagy in Huwe1-deficient neurons may be mediated via the JNK pathway under OGD/R conditions.

The current results demonstrated that the induction of autophagy was accompanied by the compensatory silencing of Huwe1 under OGD/R conditions. Whether increased autophagic activity serves a protective or harmful role is controversial. Autophagy is a double-edged sword in ischemia (24,25,68-70). Previous studies have reported that excessive autophagy in cerebral ischemia contributes to neuronal death, including autophagic cell death. Furthermore, the inhibition of excessive autophagy can attenuate cerebral ischemia-associated neuronal damage (71-73). Sciarretta *et al* (27) revealed that autophagy was beneficial during ischemia but harmful during reperfusion. In addition, a number of studies have reported that autophagy can serve as a trigger of apoptosis or necrosis, as well as act as an independent mechanism of cell death (24,53,54,74).

Silencing Huwe1 or inhibiting autophagy favors cell survival under OGD/R conditions. However, silencing Huwe1 also induces autophagy. Under OGD/R conditions, neuronal recruitment in autophagy is accompanied by Huwe1 degradation in response to I/R injury (17,42,71,75). Delgado *et al* (52) showed that a three-part signaling system involving autophagy, the UPS and apoptosis balances cell death vs. survival decisions. There are three main axes of the three-part signaling system (autophagy-apoptosis, UPS-apoptosis and autophagy-UPS), and crosstalk in the system is bidirectional (52). However, whether there is a three-part signaling system or feedback mechanism between Huwe1, autophagy and apoptosis under OGD/R conditions requires further investigation. Autophagy and apoptosis share several common modulators and signaling pathways, and may antagonize or promote one another in certain cases, such as brain injury and ischemia (73). Previous studies have suggested that JNK inhibitors effectively reduce I/R-induced cell death (76). In a previous study, it was identified that silencing Huwe1 decreased the level of p-JNK under OGD/R conditions (50). A JNK inhibitor increased the expression of autophagy-related proteins but decreased the expression levels of apoptosis-related proteins. p-JNK may be a key mediator of the antagonistic interaction between apoptosis and autophagy in response to UPS impairment in primary cortical neuronal cells (61). However, the role of p-JNK in the three-part signaling system of autophagy, the UPS and apoptosis to balance cell death vs. survival decisions in response to Huwe1 impairment under OGD/R conditions requires further investigation.

Huwe1 is involved in the ubiquitination and degradation of multiple proteins, including P53 (19). Proteasome inhibition in neurons has been shown to induce autophagy via the metabolic stabilization of the transcription factor P53 (9,61,74). Recently, it has been revealed that apoptosis signaling exhibits substantial molecular crosstalk with the UPS, as well as autophagy. Whether there is a compensatory role for autophagy following the impairment of Huwe1 via the polyubiquitination of P53, and if P53 is involved in the three-part signaling system of Huwe1, autophagy and apoptosis under OGD/R conditions is yet to be elucidated. Based on these aforementioned findings, further studies will examine the levels of the autophagy-related proteins upon the co-administration of small interfering RNA of P53 and Huwe1.

In conclusion, the present results suggested that Huwe1 silencing was accompanied by a compensatory induction of autophagy under OGD/R conditions. The JNK pathway may be a key mediator of the interaction between Huwe1 and autophagy in response to UPS impairment. However, in the context of brain ischemia, the precise mechanisms underlying the interaction between autophagy and Huwe1 require further clarification, and an additional comprehensive study is necessary.

Acknowledgements

Not applicable.

Funding

The present study was supported by The New Bud Research Foundation of West China Second University Hospital of China (grant no. kx100) and the Science and Technology Support Projects in Sichuan Province (grant no. 2019YFS0411).

Availability of data and materials

The datasets used and/or analyzed during the current study are available from the corresponding author on reasonable request.

Authors' contributions

GQH, WZ and GLH conceived and designed the study. GQH, YC and HJL performed the experiments. WZ and WMX performed the data analysis. GHQ and GLH wrote the manuscript. WZ and GLH revised the article. All authors read and approved the final manuscript.

Ethics approval and consent to participate

The present study was approved by the Animal Ethics Committee of Sichuan University (approval no. 2018013).

Patient consent for publication

Not applicable.

Competing interests

The authors declare that they have no competing interests.

References

1. Dikic I: Proteasomal and autophagic degradation systems. Annu Rev Biochem 86: 193-224, 2017.
2. Ardley HC and Robinson PA: E3 ubiquitin ligases. Essays Biochem 41: 15-30, 2005.
3. Finley D: Recognition and processing of ubiquitin-protein conjugates by the proteasome. Annu Rev Biochem 78: 477-513, 2009.
4. Zaffagnini G and Martens S: Mechanisms of selective autophagy. J Mol Biol 428: 1714-1724, 2016.
5. Martens S and Behrends C: Molecular mechanisms of selective autophagy. J Mol Biol 432: 1-2, 2020.
6. Schreiber A and Peter M: Substrate recognition in selective autophagy and the ubiquitin-proteasome system. Biochim Biophys Acta 1843: 163-181, 2014.
7. Ji CH and Kwon YT: Crosstalk and interplay between the ubiquitin-proteasome system and autophagy. Mol Cells 40: 441-449, 2017.
8. Bao X, Ren T, Huang Y, Ren C, Yang K, Zhang H and Guo W: Bortezomib induces apoptosis and suppresses cell growth and metastasis by inactivation of Stat3 signaling in chondrosarcoma. Int J Oncol 50: 477-486, 2017.
9. Lagunas-Martinez A, Garcia-Villa E, Arellano-Gaytán M, Contreras-Ochoa CO, Dimas-González J, López-Arellano ME, Madrid-Marina V and Gariglio P: MG132 plus apoptosis antigen-1 (APO-1) antibody cooperate to restore p53 activity inducing autophagy and p53-dependent apoptosis in HPV16 E6-expressing keratinocytes. Apoptosis 22: 27-40, 2017.
10. Kwon YT and Ciechanover A: The ubiquitin code in the ubiquitin-proteasome system and autophagy. Trends Biochem Sci 42: 873-886, 2017.
11. Nedelsky NB, Todd PK and Taylor JP: Autophagy and the ubiquitin-proteasome system: Collaborators in neuroprotection. Biochim Biophys Acta 1782: 691-699, 2008.
12. Fan T, Huang Z, Chen L, Wang W, Zhang B, Xu Y, Pan S, Mao Z, Hu H and Geng Q: Associations between autophagy, the ubiquitin-proteasome system and endoplasmic reticulum stress in hypoxia-deoxygenation or ischemia-reperfusion. Eur J Pharmacol 791: 157-167, 2016.
13. Nam T, Han JH, Devkota S and Lee HW: Emerging paradigm of crosstalk between autophagy and the ubiquitin-proteasome system. Mol Cells 40: 897-905, 2017.
14. Zaffagnini G, Savova A, Danieli A, Romanov J, Tremel S, Ebner M, Peterbauer T, Sztacho M, Trapannone R, Tarafder AK, *et al*: p62 filaments capture and present ubiquitinated cargos for autophagy. EMBO J 37: e98308, 2018.
15. French ME, Klosowiak JL, Aslanian A, Reed SI, Yates JR III and Hunter T: Mechanism of ubiquitin chain synthesis employed by a HECT domain ubiquitin ligase. J Biol Chem 292: 10398-10413, 2017.
16. Zhao X, D' Arca D, Lim WK, Brahmachary M, Carro MS, Ludwig T, Cardo CC, Guillemot F, Aldape K, Califano A, *et al*: The N-Myc-DLL3 cascade is suppressed by the ubiquitin ligase Huwe1 to inhibit proliferation and promote neurogenesis in the developing brain. Dev Cell 17: 210-221, 2009.
17. Zhao X, Heng JI, Guardavaccaro D, Jiang R, Pagano M, Guillemot F, Iavarone A and Lasorella A: The HECT-domain ubiquitin ligase Huwe1 controls neural differentiation and proliferation by destabilizing the N-Myc oncoprotein. Nat Cell Biol 10: 643-653, 2008.
18. The MULE/HUWE1 E3 ubiquitin ligase is a tumor suppressor. Cancer Discov 3: OF32, 2013.
19. Zhou J, Liu Q, Mao M and Tong Y: Huwe1 as a therapeutic target for neural injury. Genet Mol Res 13: 4320-4325, 2014.
20. Li Y, Luo Y, Luo T, Lu B, Wang C, Zhang Y, Piao M, Feng C and Ge P: Trehalose inhibits protein aggregation caused by transient ischemic insults through preservation of proteasome activity, not via induction of autophagy. Mol Neurobiol 54: 6857-6869, 2017.
21. Min JW, Lü L, Freeling JL, Martin DS and Wang H: USP14 inhibitor attenuates cerebral ischemia/reperfusion-induced neuronal injury in mice. J Neurochem 140: 826-833, 2017.
22. Baptista MS, Duarte CB and Maciel P: Role of the ubiquitin-proteasome system in nervous system function and disease: Using C. elegans as a dissecting tool. Cell Mol Life Sci 69: 2691-2715, 2012.
23. Eltzschig HK and Eckle T: Ischemia and reperfusion-from mechanism to translation. Nat Med 17: 1391-1401, 2011.
24. Wang P, Shao BZ, Deng Z, Chen S, Yue Z and Miao CY: Autophagy in ischemic stroke. Prog Neurobiol 163-164: 98-117, 2018.
25. Rami A and Kögel D: Apoptosis meets autophagy-like cell death in the ischemic penumbra: Two sides of the same coin? Autophagy 4: 422-426, 2008.
26. Wolf MS, Bayir H, Kochanek PM and Clark RSB: The role of autophagy in acute brain injury: A state of flux? Neurobiol Dis 122: 9-15, 2019.
27. Sciarretta S, Hariharan N, Monden Y, Zablocki D and Sadoshima J: Is autophagy in response to ischemia and reperfusion protective or detrimental for the heart? Pediatr Cardiol 32: 275-281, 2011.
28. Yan W, Zhang H, Bai X, Lu Y, Dong H and Xiong L: Autophagy activation is involved in neuroprotection induced by hyperbaric oxygen preconditioning against focal cerebral ischemia in rats. Brain Res 1402: 109-121, 2011.
29. Jiang WW, Huang BS, Han Y, Deng LH and Wu LX: Sodium hydrosulfide attenuates cerebral ischemia/reperfusion injury by suppressing overactivated autophagy in rats. FEBS Open Bio 7: 1686-1695, 2017.
30. Su J, Zhang T, Wang K, Zhu T and Li X: Autophagy activation contributes to the neuroprotection of remote ischemic perconditioning against focal cerebral ischemia in rats. Neurochem Res 39: 2068-2077, 2014.
31. Qi Z, Dong W, Shi W, Wang R, Zhang C, Zhao Y, Ji X, Liu KJ and Luo Y: Bcl-2 phosphorylation triggers autophagy switch and reduces mitochondrial damage in limb remote ischemic conditioned rats after ischemic stroke. Transl Stroke Res 6: 198-206, 2015.
32. Wei K, Wang P and Miao CY: A double-edged sword with therapeutic potential: An updated role of autophagy in ischemic cerebral injury. CNS Neurosci Ther 18: 879-886, 2012.
33. Gao L, Jiang T, Guo J, Liu Y, Cui G, Gu L, Su L and Zhang Y: Inhibition of autophagy contributes to ischemic postconditioning-induced neuroprotection against focal cerebral ischemia in rats. PLoS One 7: e46092, 2012.
34. Xu SY, Wu YM, Ji Z, Gao XY and Pan SY: A modified technique for culturing primary fetal rat cortical neurons. J Biomed Biotechnol 2012: 803930, 2012.
35. Fath T, Ke YD, Gunning P, Götz J and Ittner LM: Primary support cultures of hippocampal and substantia nigra neurons. Nat Protoc 4: 78-85, 2009.
36. Liu Z, Chen Z, Wang J, Zhang M, Li Z, Wang S, Dong B, Zhang C, Gao J and Shen L: Mouse avatar models of esophageal squamous cell carcinoma proved the potential for EGFR-TKI afatinib and uncovered Src family kinases involved in acquired resistance. J Hematol Oncol 11: 109, 2018.
37. Gertz K, Kronenberg G, Kälin RE, Baldinger T, Werner C, Balkaya M, Eom GD, Hellmann-Regen J, Kröber J, Miller KR, *et al*: Essential role of interleukin-6 in post-stroke angiogenesis. Brain 135: 1964-1980, 2012.
38. Jones SM, Novak AE and Elliott JP: Primary culture of cellular subtypes from postnatal mouse for in vitro studies of oxygen glucose deprivation. J Neurosci Methods 199: 241-248, 2011.
39. Ding B and Kilpatrick DL: Lentiviral vector production, titration, and transduction of primary neurons. Methods Mol Biol 1018: 119-131, 2013.
40. Reich A, Spering C, Gertz K, Harms C, Gerhardt E, Kronenberg G, Nave KA, Schwab M, Tauber SC, Drinkut A, *et al*: Fas/CD95 regulatory protein Faim2 is neuroprotective after transient brain ischemia. J Neurosci 31: 225-233, 2011.
41. Nagai N, Yamamoto S, Tsuboi T, Ihara H, Urano T, Takada Y, Terakawa S and Takada A: Tissue-type plasminogen activator is involved in the process of neuronal death induced by oxygen-glucose deprivation in culture. J Cereb Blood Flow Metab 21: 631-634, 2001.

42. He G, Xu W, Tong L, Li S, Su S, Tan X and Li C: Gadd45b prevents autophagy and apoptosis against rat cerebral neuron oxygen-glucose deprivation/reperfusion injury. Apoptosis 21: 390-403, 2016.
43. Zhong Q, Gao W, Du F and Wang X: Mule/ARF-BP1, a BH3-only E3 ubiquitin ligase, catalyzes the polyubiquitination of Mcl-1 and regulates apoptosis. Cell 121: 1085-1095, 2005.
44. Xu F, Gu JH and Qin ZH: Neuronal autophagy in cerebral ischemia. Neurosci Bull 28: 658-666, 2012.
45. Hale AN, Ledbetter DJ, Gawriluk TR and Rucker EB III: Autophagy: Regulation and role in development. Autophagy 9: 951-972, 2013.
46. Li W, Zhu J, Dou J, She H, Tao K, Xu H, Yang Q and Mao Z: Phosphorylation of LAMP2A by p38 MAPK couples ER stress to chaperone-mediated autophagy. Nat Commun 8: 1763, 2017.
47. Bejarano E and Cuervo AM: Chaperone-mediated autophagy. Proc Am Thorac Soc 7: 29-39, 2010.
48. Penke B, Bogár F, Crul T, Sántha M, Tóth ME and Vígh L: Heat shock proteins and autophagy pathways in neuroprotection: From molecular bases to pharmacological interventions. Int J Mol Sci 19: 325, 2018.
49. Zhang Q, Bian H, Guo L and Zhu H: Pharmacologic preconditioning with berberine attenuating ischemia-induced apoptosis and promoting autophagy in neuron. Am J Transl Res 8: 1197-1207, 2016.
50. Lalaoui N, Lindqvist LM, Sandow JJ and Ekert PG: The molecular relationships between apoptosis, autophagy and necroptosis. Semin Cell Dev Biol 39: 63-69, 2015.
51. Thorburn A: Apoptosis and autophagy: Regulatory connections between two supposedly different processes. Apoptosis 13: 1-9, 2008.
52. Delgado ME, Dyck L, Laussmann MA and Rehm M: Modulation of apoptosis sensitivity through the interplay with autophagic and proteasomal degradation pathways. Cell Death Dis 5: e1011, 2014.
53. Mariño G, Niso-Santano M, Baehrecke EH and Kroemer G: Self-consumption: The interplay of autophagy and apoptosis. Nat Rev Mol Cell Biol 15: 81-94, 2014.
54. Shi R, Weng J, Zhao L, Li XM, Gao TM and Kong J: Excessive autophagy contributes to neuron death in cerebral ischemia. CNS Neurosci Ther 18: 250-260, 2012.
55. Grasselli G and Strata P: Structural plasticity of climbing fibers and the growth-associated protein GAP-43. Front Neural Circuits 7: 25, 2013.
56. Lamb CA, Yoshimori T and Tooze SA: The autophagosome: Origins unknown, biogenesis complex. Nat Rev Mol Cell Biol 14: 759-774, 2013.
57. Chen K, Cheng HH and Zhou RJ: Molecular mechanisms and functions of autophagy and the ubiquitin-proteasome pathway. Yi Chuan 34: 5-18, 2012 (In Chinese).
58. Hu Z, Yang B, Mo X and Xiao H: Mechanism and regulation of autophagy and its role in neuronal diseases. Mol Neurobiol 52: 1190-1209, 2015.
59. Guo F, He XB, Li S and Le W: A central role for phosphorylated p38α in linking proteasome inhibition-induced apoptosis and autophagy. Mol Neurobiol 54: 7597-7609, 2017.
60. Liu C, Gao Y, Barrett J and Hu B: Autophagy and protein aggregation after brain ischemia. J Neurochem 115: 68-78, 2010.
61. Klionsky DJ, Abeliovich H, Agostinis P, Agrawal DK, Aliev G, Askew DS, Baba M, Baehrecke EH, Bahr BA, Ballabio A, *et al*: Guidelines for the use and interpretation of assays for monitoring autophagy in higher eukaryotes. Autophagy 4: 151-175, 2008.
62. Thornton C, Leaw B, Mallard C, Nair S, Jinnai M and Hagberg H: Cell death in the developing brain after hypoxia-ischemia. Front Cell Neurosci 11: 248, 2017.
63. Nozaki K, Nishimura M and Hashimoto N: Mitogen-activated protein kinases and cerebral ischemia. Mol Neurobiol 23: 1-19, 2001.
64. Wu D and Cederbaum AI: Inhibition of autophagy promotes CYP2E1-dependent toxicity in HepG2 cells via elevated oxidative stress, mitochondria dysfunction and activation of p38 and JNK MAPK. Redox Biol 1: 552-565, 2013.
65. Jia G, Cheng G, Gangahar DM and Agrawal DK: Insulin-like growth factor-1 and TNF-alpha regulate autophagy through c-jun N-terminal kinase and Akt pathways in human atherosclerotic vascular smooth cells. Immunol Cell Biol 84: 448-454, 2006.
66. Haberzettl P and Hill BG: Oxidized lipids activate autophagy in a JNK-dependent manner by stimulating the endoplasmic reticulum stress response. Redox Biol 1: 56-64, 2013.
67. Xu P, Das M, Reilly J and Davis RJ: JNK regulates FoxO-dependent autophagy in neurons. Genes Dev 25: 310-322, 2011.
68. He GQ, Xu WM, Liao HJ, Jiang C, Li CQ and Zhang W: Silencing Huwe1 reduces apoptosis of cortical neurons exposed to oxygen-glucose deprivation and reperfusion. Neural Regen Res 14: 1977-1985, 2019.
69. Wen YD, Sheng R, Zhang LS, Han R, Zhang X, Zhang XD, Han F, Fukunaga K and Qin ZH: Neuronal injury in rat model of permanent focal cerebral ischemia is associated with activation of autophagic and lysosomal pathways. Autophagy 4: 762-769, 2008.
70. Kost A, Kasprowska D, Labuzek K, Wiaderkiewicz R and Gabryel B: Autophagy in brain ischemia. Postepy Hig Med Dosw (Online) 65: 524-533, 2011 (In Polish).
71. Balduini W, Carloni S and Buonocore G: Autophagy in hypoxia-ischemia induced brain injury. J Matern Fetal Neonatal Med 25 (Suppl 1): S30-S34, 2012.
72. Lu Q, Harris VA, Kumar S, Mansour HM and Black SM: Autophagy in neonatal hypoxia ischemic brain is associated with oxidative stress. Redox Biol 6: 516-523, 2015.
73. Qiao L, Fu J, Xue X, Shi Y, Yao L, Huang W, Li J, Zhang D, Liu N, Tong X, *et al*: Neuronalinjury and roles of apoptosis and autophagy in a neonatal rat model of hypoxia-ischemia-induced periventricular leukomalacia. Mol Med Rep 17: 5940-5949, 2018.
74. Maiuri MC, Zalckvar E, Kimchi A and Kroemer G: Self-eating and self-killing: Crosstalk between autophagy and apoptosis. Nat Rev Mol Cell Biol 8: 741-752, 2007.
75. He GQ, Xu WM, Li JF, Li SS, Liu B, Tan XD and Li CQ: Huwe1 interacts with Gadd45b under oxygen-glucose deprivation and reperfusion injury in primary Rat cortical neuronal cells. Mol Brain 8: 88, 2015.
76. Kalogeris T, Baines CP, Krenz M and Korthuis RJ: Ischemia/reperfusion. Compr Physiol 7: 113-170, 2016.